ISSN (Print) 1226-1750
ISSN (Online) 2233-6656
Journal of Magnetics 23(4), 523-528 (2018) https://doi.org/10.4283/JMAG.2018.23.4.523

Comparison of the Electromagnetic Characteristics of Single-Phase Linear Oscillating Machines according to Magnetic Flux Flow

Chang-Woo Kim[1], Gang-Hyeon Jang[1], Sang-Sub Jeong[2], Junghyo Nah[1], and Jang-Young Choi[1]*

[1]*Department of Electrical Engineering, Chungnam National University, Daejeon 34134, Republic of Korea*
[2]*R&D Dept., LG Electronics, Seoul 08592, Republic of Korea*

(Received 20 June 2018, Received in final form 6 December 2018, Accepted 6 December 2018)

Linear oscillating machines are typically classified according to flux flow, as longitudinal and transverse flux type devices. In longitudinal flux linear oscillating machines, the direction of the current flow is perpendicular to the direction of the moving part, while the direction of the current flow in transverse flux linear oscillating machines is parallel to the direction of the moving part. Since the direction of the magnetic flux and the current are different in the two models, their electromagnetic characteristics can also be expected to be different. In this paper, we compare the electromagnetic characteristics of these two types of linear oscillating machines. For a fair evaluation of these characteristics, both models are designed to have the same stator outer diameter, permanent magnet volume, and no-load back electromotive force. In characterizing the devices, we analyze air gap flux density, flux linkage, and inductance, as well as the electromagnetic loss.

Keywords : electromagnetic loss analysis, linear oscillating machine, linear oscillating motor, longitudinal flux machine, transverse flux machine

1. Introduction

Linear oscillating machines (LOMs) are machines that control linear reciprocating motion using stroke cycles at a specific frequency [1]. Because of advantages such as their high transmission efficiency, simple structure, and low noise characteristics, LOMs are more suitable than traditional actuation methods that make use of rotatory motors and crankshafts, for devices such as electro-medical machines, electric hammers, linear pumps, refrigeration compressors [2-4]. LOMs can be classified according to their flux path as longitudinal flux LOMs (LFLOM) and transverse flux LOMs (TFLOM) [5]. In LFLOMs, the direction of the current flow is perpendicular to the direction of the moving part, while the direction of the current flow in TFLOMs is parallel to the direction of the moving part. Although it has been demonstrated that the use of a transverse flux structure in a machine can increase its power density and efficiency [6, 7], no studies have been conducted on the output power and efficiency of both types of LOM of the same volume, in relation to the flux path.

In this study, we compare the electromagnetic characteristics of an LFLOM and a TFLOM with equal inner core and outer core radii, and permanent magnet (PM) volumes. We employed a moving-magnet configuration for both devices, i.e., the moving parts of both the LFLOM and the TFLOM include the PMs, as this design reduces the weight of the moving part. Hence, the desired stroke can be produced through the length of the PM. This design typically has a higher power density than moving-iron-core configurations, and can be operated at comparably higher frequencies. We optimized the design of the LFLOM and the TFLOM using the above constraints, and compared the electromagnetic characteristics of the finalized designs at a specific frequency.

2. Analysis of LOMs

2.1. Topology and Features

Figure 1 depicts the models of the LFLOM and the TFLOM used in analysis, consisting of an outer core, an inner core, a coil, and a moving PM, with which the reciprocating motion occurs in the z-axis direction. The main magnetic flux of LFLOA flows from the r direction to the z direction, and the main magnetic flux of the

*Corresponding author: Tel: +82-42-821-7610
Fax: +82-42-821-8895, e-mail: choi_jy@cnu.ac.kr

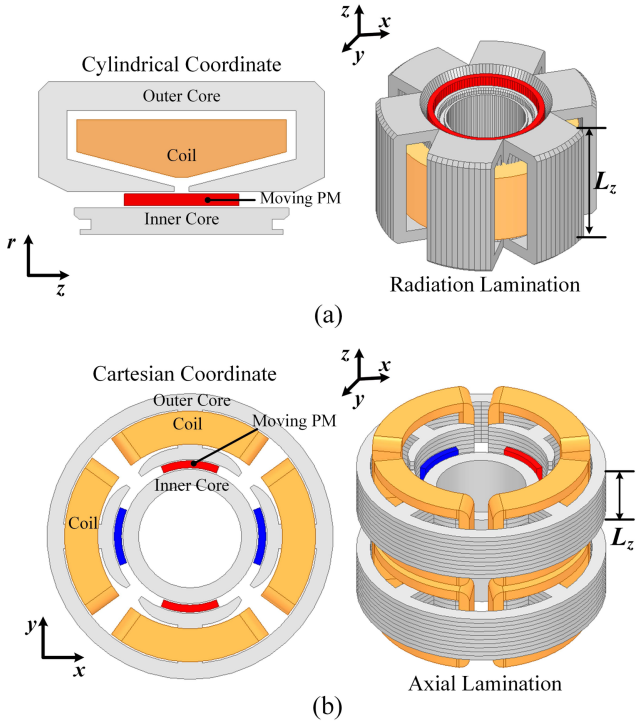

Fig. 1. (Color online) Model of (a) the LFLOM, and (b) the TFLOM.

Table 1. LOM specifications.

Parameter	Value	
Electrical steel	50PN470	
Permanent magnet	NdFeB (1.31T)	
PM conductivity	555555.5 siemens/m	
PM mass	66 g	
Parameter	LFLOM	TFLOM
PM axial length	22 mm	44 mm
PM fill factor	100 %	50 %
Outer axial length	60 mm	20 mm × 2

Table 2. Comparison of analysis results.

Parameter	LFLOM	TFLOM
Back EMF	237 V_{rms}	
Turns	400	420 × 8
Inductance	168 mH	739 mH
Input current	1 A_{rms}	
Stroke	20 mm	26 mm
Force	79.7 N	72 N
Output Power	231 W	227 W

TFLOA flows in the direction. At this time, the main current direction of the LFLOA is the direction, and the main current direction of the TFLOA is the z axis direction, so that the electromotive force is generated.

Since the LFLOM is radially laminated, the stator is assembled from multiple sections. On the other hand, the TFLOA is laminated in the axial direction and is highly manufactured. As mentioned above, in the TFLOM the direction of current flow is parallel to the direction of the moving part. As a result, the operation of this machine cannot be explained using the 2-D coordinate system. Hence, both models are analyzed using the 3-D finite element method (FEM), for more accurate characterization of their behavior. Although the radii of the outer cores and the PMs are the same, for comparative purposes, the axial length of the outer core of the TFLOM was selected to be 40 mm, in consideration of the end turn of the coil. In addition, we also increased the axial length of the PM in the TFLOM, in line with the length of the outer core, instead of reducing the drop rate to 50 %, to compensate for stroke reduction due to the end turn. The volumes of the PMs in both designs are otherwise the

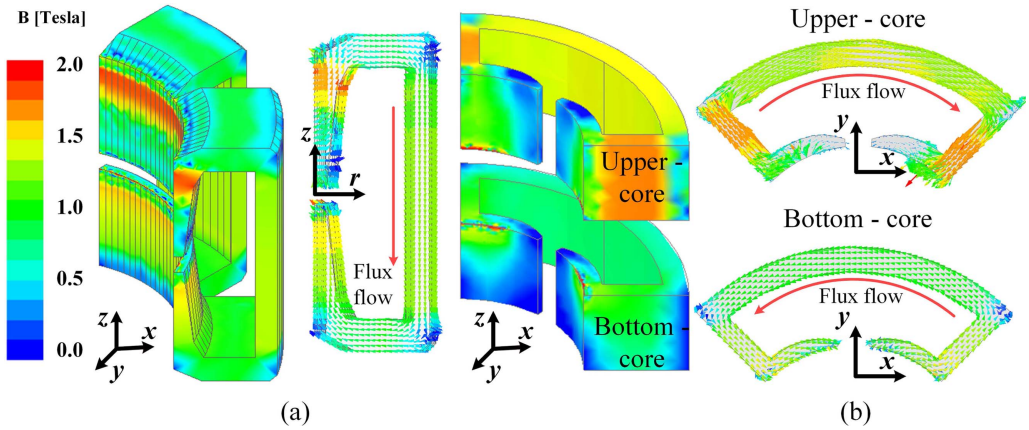

Fig. 2. (Color online) Distribution of magnetic flux density in (a) the LFLOM, and (b) the TFLOM. The red arrows indicate the direction of flux flow.

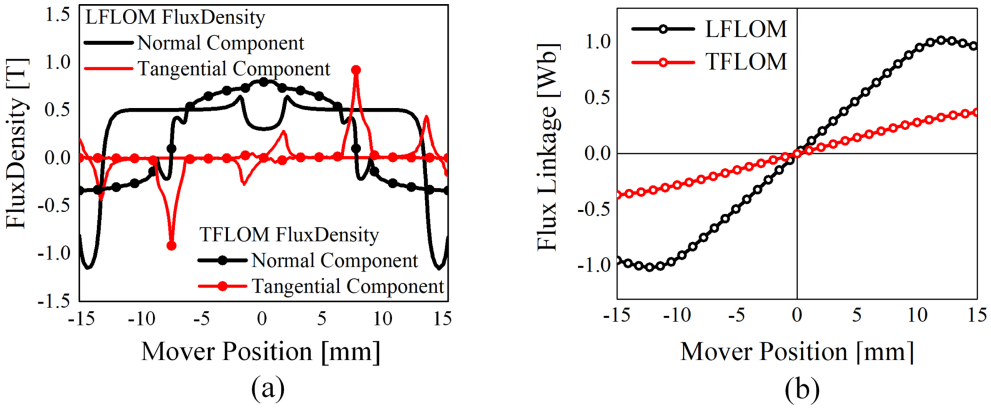

Fig. 3. (Color online) Comparison of electromagnetic characteristics in the LOMs: (a) Air-gap magnetic flux density. (b) Flux linkage.

same. Detailed specifications for both LOM models are given in Table 1. Table 2 summarizes the results of analysis performed at an applied current of 1 A_{rms}.

2.2. No-load Characteristic

Figure 2 illustrates the results of FEM analysis simulating the magnetic flux density of the LFLOM and the TFLOM. The main flux of the LFLOM varies in the z-axis direction, while the main flux of the TFLOM varies in the θ-direction. The normal and tangential components of the magnetic flux density in the air gap of both machines are shown in Fig. 3(a), while the flux linkage of both models, with respect to mover position, is shown in Fig. 3(b). We observe differences in the flux linkages of both models due to the differences in the flow of magnetic flux. The generated no-load back electromotive force (EMF) in one phase of the armature winding [8, 9] is calculated as

$$E_f = \pi\sqrt{2} f N k_{\omega 1} \Phi_f \tag{1}$$

where, f, N, $k_{\omega 1}$, and Φ_f are the respective frequency, number of turns, winding factor, and magnetic flux, of the LOM. Both models are designed such that the no-load back EMF values are the same, as illustrated in Fig. 4. Since the operating frequency and magnetic flux of both models are the same, the number of turns is adjusted to ensure this condition is met. This adjustment means that the inductance of the TFLOM is high. The inductance can be calculated as follows [10].

$$L_s = \frac{\Phi_f}{I} \tag{2}$$

The magnetic flux (Φ_f) that links the N-turn armature coil can be calculated as the sum of the fluxes inside each turn. Therefore, the inductance difference is caused by the difference in the number of turns. The analysis results of the two LOMs are shown in Table 2.

2.3. Force Characteristic

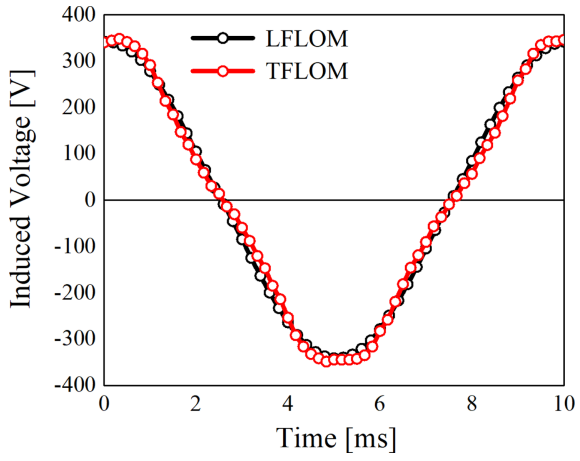

Fig. 4. (Color online) Comparison of back EMF in the LFLOM and the TFLOM.

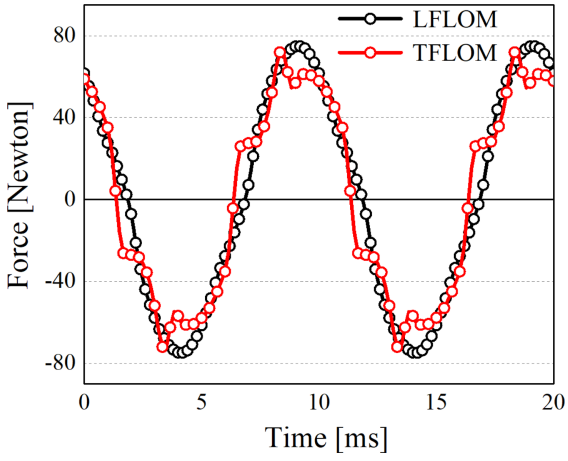

Fig. 5. (Color online) Comparison of the magnetic force generated by the LFLOM and the TFLOM.

The magnetic force generated by the reciprocating motion of the moving parts of the LOMs. Fig. 5 shows the magnetic force, **F**, calculated by FEM, and this force in the FEM is calculated using the Maxwell stress tensor [11] as below:

$$\mathbf{F_z} = \frac{1}{\mu_0}\int_0^l \int_0^{2\pi} \mathbf{B}_n \mathbf{B}_t r d\theta dz \tag{3}$$

where $\mathbf{B_n}$ and $\mathbf{B_t}$ are the time-dependent normal and tangential components of the magnetic flux density, respectively. We observe that the force waveform of the LFLOM is sinusoidal. In contrast, the force waveform of the TFLOM is distorted as a result of the motion of the PM through the end turn.

3. Electromagnetic Loss

The electromagnetic loss of an LOM typically consists of copper loss, iron loss, and PM loss. In this paper, we present analytical methods for evaluating each component, for a detailed comparison of the output power and efficiency of the two LOM models. The output characteristics of both models are summarized in Table 3.

3.1. Copper loss

The copper loss of an LOM is calculated from the phase resistance and current as,

$$P_{cu} = R_{ph} I_{rms}^2 \tag{4}$$

where P_{cu}, and I_{rms} are, respectively, the copper loss and effective phase current of the LOM, owing to the operating load condition. R_{ph} is the phase resistance, and is calculated as follows:

$$R_{ph} = \rho_0 \left[1 + \alpha_r (T - T_0)\right] \frac{l_w}{S_c} \tag{5}$$

In (5), ρ_o is the resistivity of copper at room temperature, T_0, αr is the temperature coefficient of resistivity, T is about 80 ºC in the operational temperature of the LOM

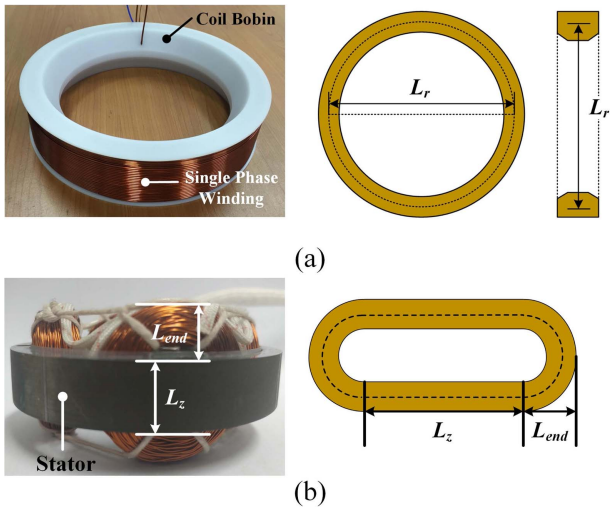

Fig. 6. (Color online) Stator winding model for calculating the single-coil length in (a) the LFLOM, and (b) the TFLOM.

at the rated condition, and l_w and *Sc* are the total length of the coil winding and the cross-sectional area of the coil, respectively. l_w can be calculated by multiplying the single-coil length of the LOM by the number of turns. Hence, it is possible to calculate the copper loss according to the current of both models. Fig. 6(a) shows a stator winding model for calculating the single-coil length of the LFLOM, where L_r is the average diameter of the coil. The single-coil length, l_{LFLOM}, can be calculated as follows:

$$l_{LFLOA} = 2\pi (L_r / 2) \tag{6}$$

Figure 6(b) shows a stator winding model for calculating the single-coil length of the TFLOM, where L_z is the axial length of the device and Lend is the length of the end turn. Hence, the single-coil length, l_{TFLOM}, can be calculated as follows:

$$l_{TFLOA} = 2L_z + 2\pi L_{end} \tag{7}$$

Using (5), (6), and (7), we calculated the phase resistance of the LFLOM to be 2.1 Ω, and the phase

Table 3. Comparison of output characteristics.

Parameter	LFLOM			TFLOM		
Input current	1 A_{rms}	3 A_{rms}	5 A_{rms}	1 A_{rms}	3 A_{rms}	5 A_{rms}
Phase resistance		2.1 Ω			17 Ω	
Force	79.7 N	220 N	323 N	72 N	153 N	212 N
Output power	231 W	674 W	1024W	227 W	583 W	825 W
Copper loss	2.1 W	19 W	52 W	17 W	154 W	427 W
PM loss	16 W	45 W	89 W	3 W	4.7 W	8.4 W
Core loss	6.8 W	13 W	22 W	6.5 W	21 W	35 W
Efficiency	90 %	90.1 %	86 %	89.7 %	76.5 %	64 %

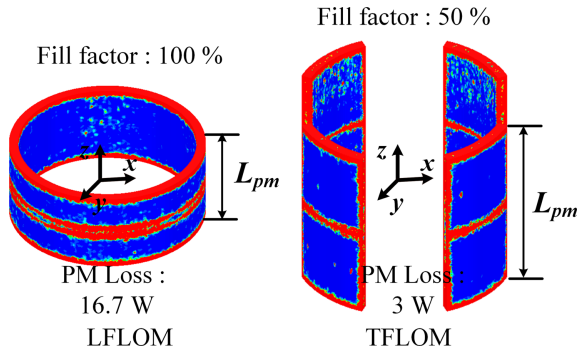

Fig. 7. (Color online) Comparison of PM loss in the LFLOM and the TFLOM.

resistance of TFLOM to be 17 Ω. The copper losses calculated based on these resistances are summarized in Table 3.

3.2. PM loss

The eddy current loss, P_{PM}, induced in the PMs is calculated as follows [12]:

$$P_{PM} = \frac{\omega_n}{2\pi} \int \int \frac{J_e^2}{\sigma} dVdt \tag{8}$$

where J_e, σ are the RMS value of the eddy current density in the PMs, and conductivity of the PMs. Although PMs of the same volume are used in both models, these are divided in the TFLOM, reducing the PM loss of this device.

3.3. Core loss

Core losses in PM machines are calculated based on the Steinmetz equation. In general rotating PM machines, it is necessary to carry out the analysis considering the rotating magnetic field and the alternating magnetic field. However, analysis of the magnetic field behavior of the linear PM machine shows that it is mostly composed of the alternating magnetic field [13]. Therefore, the iron loss was calculated as follows [14] :

$$P_{core} = P_h + P_e + P_a = k_h f_c B_c^{n_{st}} + k_e f_c^2 B_c^2 + k_a f_c^{1.5} B_c^{1.5} \tag{9}$$

In (9), P_h, P_e, and P_a are the hysteresis loss, eddy current loss, and excess loss, respectively, and k_h, k_e, and k_a, are respectively, the hysteresis loss coefficient, the eddy current loss coefficient, and the excess loss coefficient, which are estimated using a curve fitting method. Finally, n_{st} is the Steinmetz constant. f_c and B_c are the frequency and flux density in the core, respectively. To reduce eddy current losses in electrical steel sheets, the LFLOM is laminated in the axial direction and the TFLOM is laminated in the radial direction. We calculated similar values for core loss in both LOMs, as summarized in Table 3.

3.4. Efficiency

Figure 8(a) and (b) show the force and efficiency of the LOMs, respectively, with respect to the applied current. A more detailed summary of these results is given in Table 3. Although the core loss in both types of device is similar, the difference between copper loss and PM loss is large. In the case of the LFLOM, which uses a barrel magnet, the PM loss is high, whereas with the TFLOM, where a large number coils are used, copper loss is high. As copper loss is proportional to the square of the current, the output power and efficiency of the TFLOM decrease as the current increases.

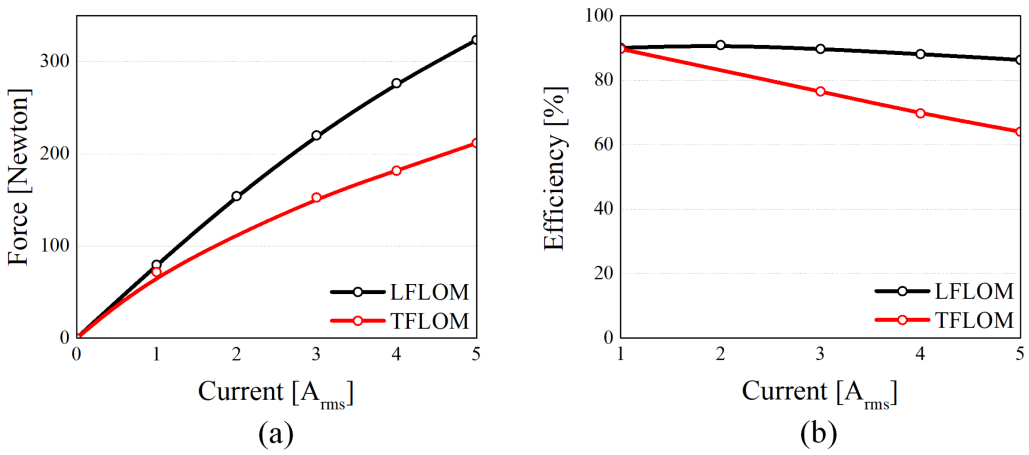

Fig. 8. (Color online) Comparison of the output characteristics of the LFLOM and the TFLOM: (a) magnetic force and (b) efficiency.

4. Conclusion

In this paper, we compared the behavior of an LFLOM and a TFLOM under the same conditions. We observed the electromagnetic characteristics of the two models, including the magnetic flux density, leakage flux, back EMF, and magnetic force. For a comprehensive comparison of the electromagnetic efficiency, we analyzed the copper loss, the PM loss, and the core loss of both models. With the TFLOM, the PM loss is relatively small since the PMs are split. However, because of the length of the coil, the copper loss is larger with this device than it is with the LFLOM. Hence, although the TFLOM can produce similar forces and electromagnetic efficiencies as an LFLOM at a low current, it is not suitable for use as a high-capacity LOM that requires a large input current.

Acknowledgements

This work was supported by the Basic Research Laboratory (BRL) of the National Research Foundation (NRF-2017R1A4A1015744) funded by the Korean government.

This work was supported by the Development of Core Technology for Large capacity Francis turbine/Synchronous generator design and Diagnostic system creating New Market of the Korea Institute of Energy Technology Evaluation and Planning (KETEP) grant funded by the Korea government Ministry of Knowledge Economy (No. 20163010060350).

References

[1] W. Jiabin, D. Howe, and L. Zhengyu, IEEE Trans. Ind. Appl. **57**, 327 (2010).
[2] Taib Ibrahim, W. Jiabin, and D. Howe, IEEE Trans. Magn. **44**, 4361 (2008).
[3] Z. Q. Zhu and X. Chen, IEEE Trans. Magn. **45**, 1384 (2009).
[4] Z. Q. Zhu, X. Chen, D. Howe, and S. Iwasaki, IEEE Trans. Magn. **44**, 3855 (2008).
[5] Hao Chen, Rui Nie, and Wenju Yan, IEEE Trans. Magn. **53**, 8205804 (2017).
[6] Yuqiu Zhang, Qinfen Lu, Minghu Yu, and Yunyue Yu, IEEE Trans. Magn. **48**, 1856 (2012).
[7] Ping Zheng, Shaohong Zhu, Bin Yu, Luming Cheng, and Yuhui Fan, IEEE Trans. Magn. **51**, 8111304 (2015).
[8] Jacek F. Gieras, Zbigniew J. Piech, and Bronislaw Z. Tomczuk, Linear Synchronous Motors, CRC Press (2011) pp 111-115.
[9] Jiabin Wang, Geraint W. Jewell, and David Howe, IEEE Trans. Magn. **35**, 3 (1999).
[10] B. Tomczuk, G. Schroder, and A. Waindok, IEEE Trans. Magn. **43**, 7 (2007).
[11] K. J. Meesen, J. J. H. Paulides, and E. A. Lomonova, IEEE Trans. Magn. **49**, 536 (2013).
[12] K. Yamazaki, Y. Fukushima, and M. Sato, IEEE Trans. Ind. Appl. **45**, 1334 (2009).
[13] J. M. Kim, Ph.D. Thesis, Chungnam National University, Korea (2017).
[14] K. Yamazaki and Y. Fukushima, IEEE Trans. Magn. **46**, 3121 (2010).